Journal of the European Ceramic Society 37 (2017) 705–713

Contents lists available at www.sciencedirect.com

Journal of the European Ceramic Society

journal homepage: www.elsevier.com/locate/jeurceramsoc

Liquid phase flash sintering in magnesia silicate glass-containing alumina

Mattia Biesuz[a,*], Vincenzo M. Sglavo[a,b]

[a] University of Trento, Department of Industrial Engineering Via Sommarive 9, 38123 Trento, Italy
[b] INSTM, Trento Research Unit Via G. Giusti 9, 50121 Firenze, Italy

ARTICLE INFO

Article history:
Received 19 June 2016
Received in revised form 17 August 2016
Accepted 30 August 2016
Available online 1 September 2016

Keywords:
Flash sintering
Liquid phase sintering
Alumina
Glass softening

ABSTRACT

Magnesia silicate glass-containing alumina was flash sintered using an E-Field in the 500–1500 V/cm range. The addition of glass allows to reduce the current needed for densification and improves the shrinkage obtained during field-assisted sintering process. This behaviour is related to the different sintering mechanisms involved in the two materials, i.e. solid state sintering for pure alumina and liquid phase sintering for glass-containing alumina.

The estimated activation energy for conduction during flash sintering is compatible with ionic diffusion in silicate melt. Moreover, evidence of magnesium diffusion toward the cathode is recorded. The estimated sample temperature is in almost all cases lower than 1355 °C, which is the temperature at which the first liquid is formed in the ternary system MgO-SiO_2-Al_2O_3. Finally, it is shown that the application of an E-Field accounts for efficient liquid phase sintering at temperatures at which it cannot be reproduced conventionally.

1. Introduction

Field Assisted Sintering (FAS) techniques represent one of the more promising routes for reducing sintering time and temperature of ceramic materials. Several research studies have been carried out in the last five years specifically on Flash Sintering (FS), showing that the densification process can be completed in just a few seconds at temperatures much lower than those required for conventional procedures. FS has proved to be a very efficient and effective sintering technique in ceramics with different electrical properties: high temperature ionic [1–12] and protonic [13] conductors, semiconductors [14], composites [15–17], electronic conductors [18–20] and insulators [21,22]. Such unusual behaviour is also followed by an anomalous drop in material resistivity. Although a thermal runaway from Joule heating has been proven to occur along flash sintering [4,17,23], the mechanisms leading to densification and the electrical behaviour are still not completely clear.

Very recent research has shown that the softening temperature of glass can be drastically reduced by the application of an electric field [24,25]. Such anticipated electric field-induced softening has been observed in some alkali-silicate glasses under DC polarization [24]. In these materials a non-conventional conduction behaviour also was observed, showing a sharp and unexpected increase of electrical conductivity of the glass.

Nowadays, many traditional and advanced ceramics are consolidated using a liquid-phase sintering process whereby the presence of a relatively small amount of liquid at high temperature promotes additional densification mechanisms [26].

A recent work by Gonzales-Julian et al. [27] has shown that the application of a moderate electrical field enhances the densification process of lime-silicate glass-containing alumina at high temperature (1450 °C).

The goal of the present work is to extend the application of flash sintering – used so far only on materials characterized only by the presence of crystalline phases – to a very common and technologically important ceramic system, namely magnesia-silicate glass-containing alumina. The specific aim was to explore the combined effect of electric field-induced glass softening and flash sintering to decrease sintering temperature and time of α-Al_2O_3 containing 10 wt% magnesia-silicate glass.

2. Experimental procedure

Nearly pure α-alumina (Almatis CT3000SG, $d_{50} = 0.6\,\mu m$) was used in the present work. The nominal composition is: Al_2O_3

* Corresponding author.
E-mail addresses: mattia.biesuz@unitn.it (M. Biesuz), vincenzo.sglavo@unitn.it (V.M. Sglavo).

http://dx.doi.org/10.1016/j.jeurceramsoc.2016.08.036
0955-2219/

99.8 wt% - MgO 0.04 wt% - Na_2O 0.03 wt% - Fe_2O_3 0.015 wt% - SiO_2 0.015 wt% - CaO 0.015 wt%. The magnesia-silicate glass was produced by sol-gel method from TEOS (Sigma Aldrich) and magnesium nitrate hexahydrate (Sigma Aldrich) as silica and magnesia precursor, respectively. TEOS and magnesium nitrate were dissolved in 2-propanol; then, 10% NH_4OH water solution was added for TEOS hydrolysis. The resulting suspension was dried overnight at 100 °C. The obtained powder was then added to alumina and ball milled in 2-propanol for 3 h. The suspension was dried and calcined in a muffle furnace under static air using a heating rate of 10 °C/min up to 750 °C (soaking time = 30 min). The nominal composition of the powder was α-Al_2O_3, 90 wt%, SiO_2 8 wt%, MgO 2 wt%. Pure alumina powder was used also, for comparison.

The powder was uniaxially pressed in dog-bone-like samples using 7 wt% water as binder. The gage cross-section of the specimens was around 3 × 3 mm^2. One small hole was produced on each flared region of the dog-bone sample for electrical connection. The green samples were placed into an alumina dilatometer (Linseis L75) and connected by two platinum wires to a DC power supply (Glassman EW series) and a multimeter (Keithley 2100). A drop of platinum paste (Sigma Aldrich) was added into the holes in order to improve electrical contact between the green body and the wires.

The samples were heated at a rate of 20 °C/min. Once the temperature reached 300 °C, the power supply was turned on and the system started to work in voltage control. Fields in the 500–1500 V/cm range were used for the treatments. When the set current limit was reached, the system was left to work for 2 min in current control; then, power supply and furnace were shut down. Nominal current density in the range of 0.6–2 mA/mm^2 was applied to the magnesia-silicate glass-containing alumina (MgGCA) samples; pure alumina (A) specimens were studied only at 2 mA/mm^2, for comparison.

In order to point out the effect of glass composition on the process, pure silica glass was produced from TEOS hydrolysis and mixed to alumina powder, thus obtaining a silica glass-containing alumina (SiGCA) with nominal composition: α-Al_2O_3 90 wt%, SiO_2 10 wt%. This material was tested using 1000 V/cm, only.

The samples' microstructure was characterized via SEM (Jeol JSM-5500). The apparent density was determined by Archimede's method, using an analytical balance with sensitivity ±0.0001 g (Gibertini). For this analysis only the gage of the dog-bone samples (where the current density can be easily calculated) was taken into account. EDS analysis was carried out using Jeol IT300 SEM equipped with XFlash 630 M detector (Bruker Quantax).

3. Results and discussion

3.1. Densification behaviour and microstructural analysis

Both the magnesia-silicate glass-containing alumina and the pure alumina samples were flash sintered under fields exceeding 500 V/cm. Fig. 1 shows the dilatometric plots for the two materials using 2 mA/mm^2 nominal current limit. One can clearly observe that the glass addition accounts for a drastic increase in sintering rate, and this leads to greater shrinkage upon sintering. This is probably due the formation of a ternary liquid phase that enhances the densification mechanisms. Therefore, the results show clearly that flash sintering is a very effective technique for improving also the densification of glass-containing ceramic systems. An exception is represented by the samples sintered under 1500 V/cm; in such cases the current limit in the MgGCA system is reached at a very low furnace temperature (650–750 °C) but no significant densification and shrinkage are achieved. Although a definitive explanation can not be drawn, this could be accounted for by the very low furnace temperature, which results also in a lower sample temperature during the flash (for details see the power balance equation in refs [2,4,22]).

The dilatometric curves for the MgGCA samples show two shrinking events. The first one occurs at a lower temperature and produces a moderate shrinkage of the sample (~2%). This is quite likely associated to softening in the vitreous phase, which allows for the rearrangement of the solid alumina particles. In fact, particles rearrangement takes place during the very first steps of liquid phase sintering process as described by Rahaman [26]. The temperature at which such phenomenon is observed decreases with the E-Field (Fig. 1) and it will be described more in detail in section 3.2. The associated shrinkage seems to be only slightly influenced by the E-field, as shown in Fig. 1. Therefore, one can state that the E-field application lowers the temperature needed for particle rearrangement, but its magnitude is, at a first approximation, independent from the field.

The second shrinkage event observed (Fig. 1) during liquid phase sintering occurs at higher temperature and is responsible for most of the shrinkage; it is due to "*Densification. . .by solution-precipitation*" [26]. This phenomenon is strongly influenced by the applied field. During FS it occurs once the current limit is reached, its onset temperature depending from the field strength; the sintering rate (i.e. the slope of the dilatometric plots) is much higher in FS than in conventional sintering (Fig. 1).

Conversely, SiGCA does not flash sinter under E-field equal to 1000 V/cm. The maximum furnace temperature for such material was limited to 1220 °C because of sparkling that occurred during the experiments. This is suggesting that the glass composition plays an important role on the FAS behaviour of the material. The presence of magnesium enhances the conductivity of the glassy phase thus allowing the flash sintering phenomenon; conversely, pure silica glass is extremely resistive and flash sintering can not be observed.

The porosity and density data collected from the flash sintered bodies (MgGCA) are shown in Fig. 2. One can notice that the current density is controlling the densification behaviour and using only 2 mA/mm^2 the apparent porosity of the MgGCA system is reduced to less than 4%. Moreover, especially if low currents are applied, there is a quite strong correlation between the applied voltage and the physical properties of the sintered bodies. In particular, the material becomes denser by decreasing the voltage, as a result of the higher onset temperature for flash sintering. As a matter of fact, the samples treated under lower fields are already partially shrunk and thus densified when the current limit is reached.

No significant differences are observed among samples treated using different fields especially when higher currents are used. The samples treated using 1500 V/cm are always not densified and the behaviour is weakly related to the applied current. In fact, by increasing the nominal current density from 0.6 to 2 mA/mm^2, the differences in terms of bulk density and open porosity appears negligible.

Fig. 3 compares bulk density and open porosity for MgGCA and A systems. As expected from the dilatometric tests results, densification is enhanced by the addition of glass to alumina powder. In particular, MgGCA samples feature much lower open porosity. The differences are less evident in terms of bulk density, although one should consider that the theoretical density of the two materials is not the same: assuming that, after sintering, the glassy phase load is still 10 wt%, if densities of 2.20 and 3.95 g/cm^3 are considered for glass and alumina, respectively, then the theoretical density of MgGCA material is 3.66 g/cm^3, lower than that of pure alumina (3.95 g/cm^3). An exception is represented, once again, by the MgGCA samples sintered under 1500 V/cm: such specimens are not dense and feature a relevant amount of open pores.

Fig. 4 shows the fracture surface of pure alumina and magnesia-silicate glass-containing alumina specimens. All SEM micrographs

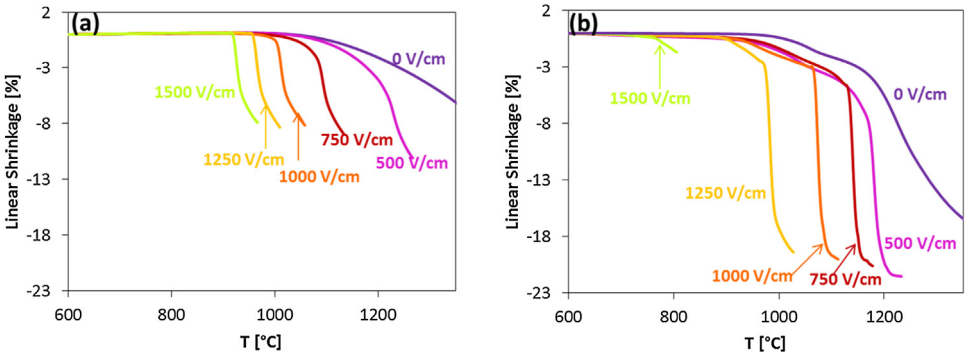

Fig. 1. Dilatometric plot for pure alumina (a) and magnesia-silicate glass-containing alumina (b) samples sintered under different electric fields and current limit of 2 mA/mm^2.

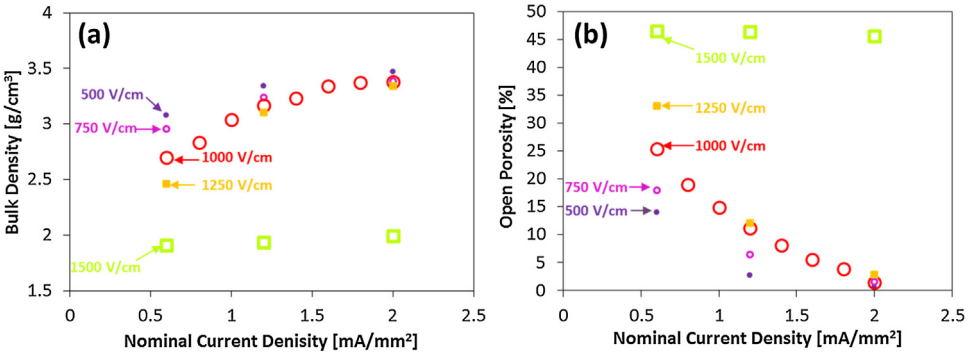

Fig. 2. Bulk density (a) and open porosity (b) for MgGCA sintered bodies as a function of current density.

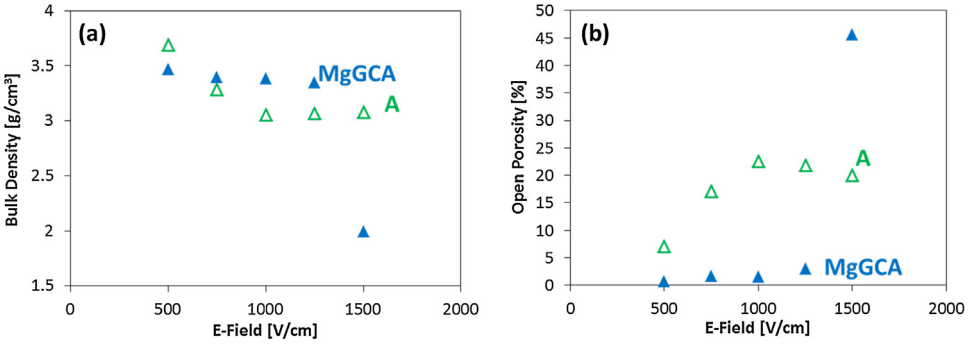

Fig. 3. Bulk density (a) and open porosity (b) for glass-containing alumina (MgGCA) and pure alumina (A) sintered bodies as a function of current density.

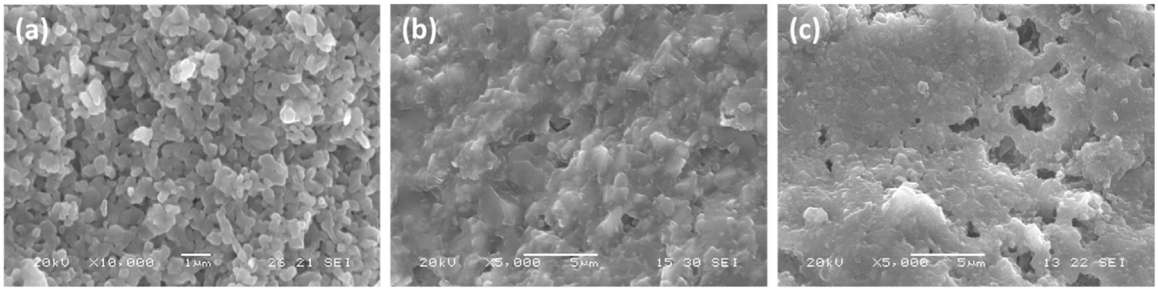

Fig. 4. SEM micrographs of the fracture surface of pure alumina (a), magnesia-silicate glass-containing alumina sample treated under 1000 V/cm and 2 mA/mm^2 (b) and MgGCA sample flash sintered under 1000 V/cm with lower current density (0.6 mA/mm^2) (c).

refer to the central part of the gage portion of the dog bone sample. If the same current density is used, the glass-containing material is denser than pure alumina and characterized by more limited porosity, in good agreement with the density measurements. This means that with the glass addition it is possible to achieve the same densification using lower current density and power dissipation. This has a significant beneficial role because it allows to avoid some technological problems related to electrode melting, partial reduction of the material and sparkling, which are often observed in the case of high current applications. In addition, the two materials

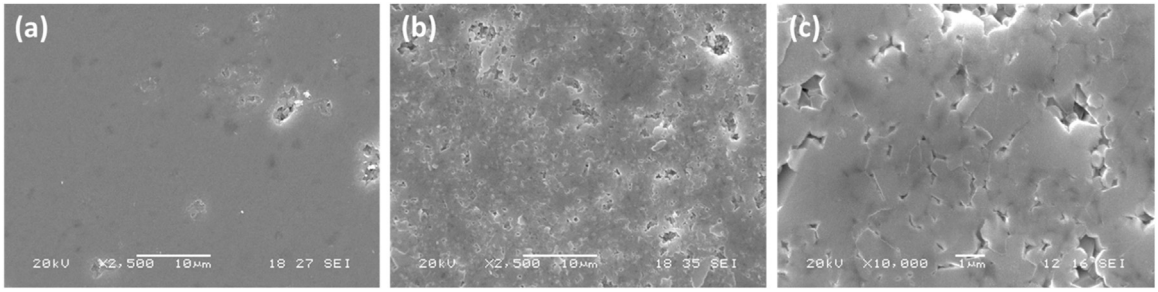

Fig. 5. SEM micrographs of polished (a) and polished and HF etched (b,c) surface (at different magnification) for MgGCA samples treated using 1000 V/cm and 2 mA/mm^2.

show a very different microstructure. The fracture mechanism is intergranular and transgranular in A and MgGCA system, respectively, this being associated to different densification mechanisms: it should not come as a surprise that the micrographs resemble solid state sintering – produced structure for pure alumina, while for magnesia-silicate glass-containing alumina the activation of a glassy phase upon densification shall be considered. Such evidence confirms that a liquid is formed during the sintering process of MgGCA, which is responsible for the differences observed in the densification behaviour. Another likely event is that, even when the current density is reduced down to 0.6 mA/mm^2 in MgGCA (Fig. 4(c)), a liquid phase sintering is observed. Indeed, the current density decrease changes the material microstructure, the samples treated with lower currents being characterized by a larger amount of pores (Fig. 4(b,c)), as expected by the density evolution described in Fig. 2. However, in all the cases, the fracture pattern suggests a liquid phase sintering mechanism.

Additional features can be analysed from observing polished and HF-etched cross-sections from MgGCA samples. Etching was carried out using 10% HF water solution for 25 s. Fig. 5 compares the polished surface before and after HF-etching: it is possible to observe that a large amount of porosity is opened by etching. This suggests that a large amount of glassy phase is present in the sintered sample; in other words, the glass is not completely crystallized during the sintering process. It should also be pointed out that pores that open upon etching are characterized by a very stretched and sharp shape (Fig. 5(c)). This clearly indicates that the glass was able to flow between the alumina grains during the sintering process. This confirms that in the glass-containing material a liquid phase flash sintering process took place.

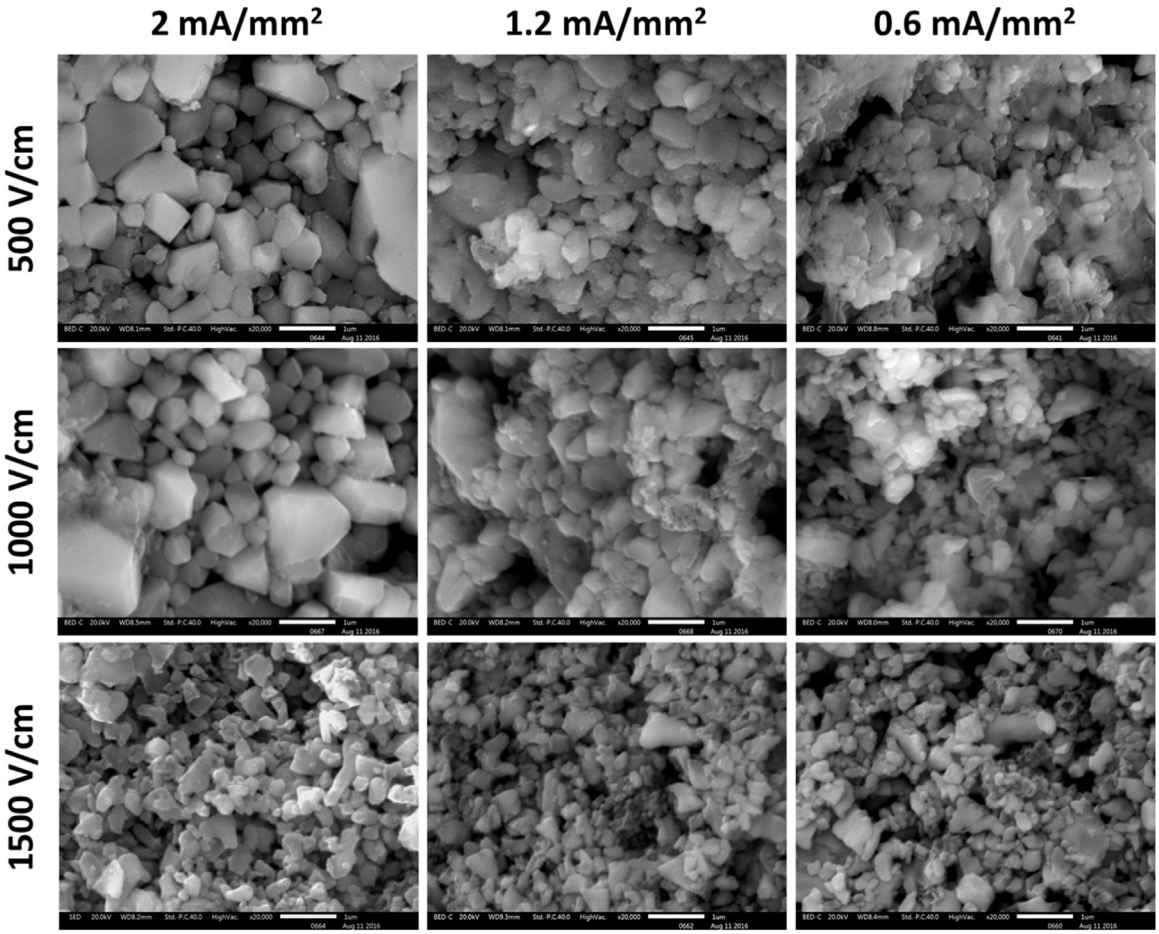

Fig. 6. SEM-BSE micrographs of HF etched MgGCA samples treated using different fields strength and current densities. The pores located at the grain boundaries are a result of the glass dissolution during the etching process.

Table 1
Grain size (nm) as a function of field strength and current density.

		J [mA/mm²]		
		0.6	1.2	2
E [V/cm]	500	359 ± 58	453 ± 52	532 ± 98
	750	321 ± 42	411 ± 85	492 ± 65
	1000	315 ± 35	470 ± 70	518 ± 40
	1250	317 ± 70	396 ± 60	502 ± 54
	1500	315 ± 25	345 ± 47	402 ± 51

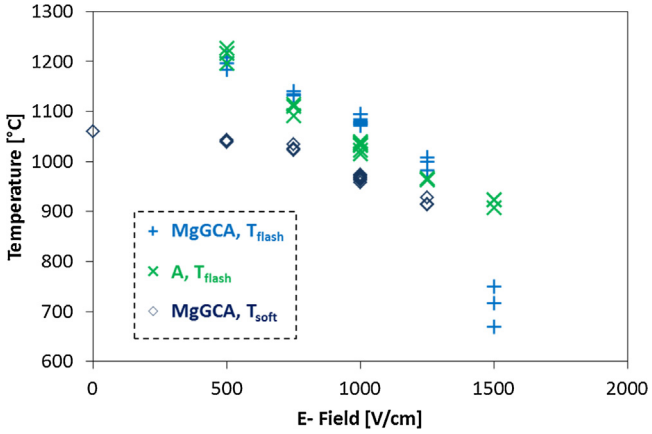

Fig. 7. Onset temperature for flash sintering for pure alumina and MgGCA. The temperature at which the maximum shrinkage rate is reached during glass softening is also shown.

Fig. 6 and Table 1 provide an overview of the grain size evolution as a function of the processing parameters (E and J). All the results are referred to the central part of the gage section of HF etched samples. First of all one can notice that the grains are mainly equiaxial and the average grain size is in all the cases sub-micrometric as a result of the very short processing time. So, even if the densification phenomena were very effective during the process a very limited grain growth took place.

A second consideration is related to the fact that the current density is the key parameter controlling the grain size (i.e. higher current limit leads to coarser microstructure). This could be a result of the fact that the sample temperature reached during the steady stage of FS is controlled by the current density, being the system in current control.

The effect of the field strength on grain size is much less pronounced. In particular, the samples treated with field in the range 500–1250 V/cm do not show consistent microstructural differences. An exception is, once again, represented by the specimens treated with 1500 V/cm which are characterized by the presence of grains substantially smaller and by a very weak densification, as previously discussed.

Finally, in the case of the specimens treated with higher currents (2 mA/mm²) some large grains (1000 nm or more) can be sporadically observed. This is not surprising since abnormal grain growth have been already reported in the scientific literature for alumina sintered with glass-formers addition [28].

3.2. Sintering temperature and electrical behaviour before FS

The relationship between the onset temperature for FS and the applied voltage is shown in Fig. 7. One can observe that in the A system the behaviour is regular and it has been successfully modelled in a previous work using the thermal runaway model [22]. Conversely, MgGCA material behaves in a quite irregular way: under a higher field (1500 V/cm), the sintering event is anticipated with respect to pure alumina by more than 200 °C. However, by decreasing the voltage, glass containing samples are flash sintered at higher temperatures.

At low temperatures (generally less than 970–870 °C), glass-containing alumina powder is more conductive than pure alumina powder and this results in higher specific power dissipation in the MgGCA system, as shown in Fig. 8(a).

Different activation energy for conduction was also estimated from the power dissipation plots, from the slope in the low temperature region characterized by a linear-like behaviour (right portion of the diagrams in Fig. 8). In particular, the activation energy was 0.7 ± 0.1 and 1.2 ± 0.2 eV for MgGCA and A samples, respectively. This suggests that at low temperature the glassy phase is more conductive than alumina and plays a central role in the charge transport mechanisms. One can see that the calculated activation energy is much lower than the literature data reported for Si^{4+}, O^{2-} and Mg^{2+} diffusion in silicate minerals and glasses, these ranging between 2.0 and 4.3 eV [29–33]. In addition, the band gap for electron promotion in fused silica is much higher (8.3 eV) [34]. The reasons for such unexpected behaviour can be related to some characteristics of the glassy phase. One should consider that the glass was produced by sol-gel method and therefore the obtained material is quite different from conventional glass. Other authors have already pointed out that glasses obtained by sol-gel methods are characterized by lower activation energy for ionic species diffusion, their diffusivity being more than one order of magnitude higher than that of bulk vitreous materials [35].

At higher temperatures, usually in the 820–1000 °C range, the power dissipation plot of the glass-containing samples presents a certain instability. First, the slope of the curve starts increasing (as it happens just before FS) but after a few minutes the concavity turns downward (Fig. 8). In this temperature range, the MgGCA system becomes more resistive (Fig. 8(a)) when compared to pure alumina and it results in a delayed FS event for the glass-containing samples. This phenomenon is probably related to a partial crystallization of the glassy phase with the formation of Enstatite (magnesium silicate), which could be responsible for a glass resistivity increase.

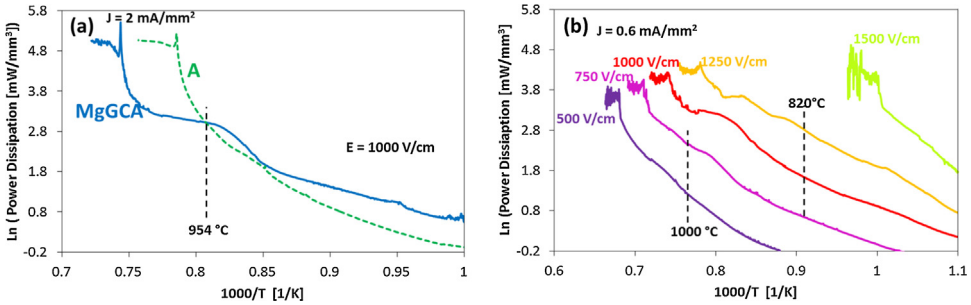

Fig. 8. Specific power dissipation as a function of the furnace temperature: (a) comparison between pure alumina and glass-containing material flash sintered under 1000 V/cm and 2 mA/mm²; (b) power dissipation during flash sintering of MgGCA samples treated under different fields using a current limit of 0.6 mA/mm².

The formation of Enstatite at 860 °C was confirmed by XRD and DSC analysis.

If a very high field is applied (1500 V/cm), the slope of the power dissipation plot for MgGCA specimens changes (Fig. 8(b)). In this case, the activation energy was estimated to be 1.6 eV, significantly higher than that measured under lower voltages (0.7 eV). This indicates the presence of a non-linear conduction behaviour and a "field-induced" activation of different charge transport mechanisms. The enhancement in conductivity has already been reported and studied using very high fields in several glassy oxide systems [36,37]. One can also observe that the current limit is reached before the previously discussed partial crystallization of the glass. This means that the material is flash sintered in the temperature range in which the glass is much more conductive than alumina. The fact that alumina is probably not completely involved in charge transport mechanisms is another reason that can be claimed for explaining the limited densification of such specimens.

Finally, Fig. 7 shows that the field also influences the temperature at which the maximum shrinkage rate is reached during glass softening, as a result of particles rearrangement. This parameter is obviously related to the glass-softening temperature and it is possible to refer to it as an indicator of the amorphous phase behaviour. In particular, in the tests carried out at 750–1250 V/cm, this reference temperature is only anticipating the flash sintering by 80–110 °C. Therefore, it behaves in a way similar to that of the onset temperature for FS. The correlation between the temperature at which the maximum shrinkage rate is reached during glass softening and the applied field could be accounted for by the Joule heating phenomenon that always precedes the achievement of the current limit. Nevertheless, at 750 V/cm the reference temperature reaches a plateau and it changes by just a few degrees when the field decreases down to 0 V/cm. This means that the glassy phase behaviour before FS is independent from the applied field in the range 0–750 V/cm. It may suggest that the glass is not particularly involved in charge transport phenomena in the temperature range between the described crystallization and FS.

3.3. Electrical behaviour during FS

Material resistivity was estimated during FS. In particular, the data collected in the second minute after the FS event were analysed in order to make sure that the system was stable enough and that the specimen temperature was relatively constant. The real resistivity of the system was calculated considering that in all specimens a certain amount of porosity was still present during the process. All values were estimated under the following hypothesis:

i Most of the densification occurs in the first minute after FS;
ii The porosity is homogenously distributed;
iii The density of the material can be approximated to that previously measured.

Fig. 9 shows resistivity as a function of the estimated sample temperature. The resistivity ($\rho_{(T)}$) in ceramic oxide materials typically scales with temperature according to the following equation:

$$ln\left(\rho_{(T_S)}\right) = \ln(\rho_0) + Q/RT_S \quad (1)$$

where ρ_0 is a pre-exponential constant, Q the activation energy for conduction, R the universal gas constant and T_S the sample temperature.

The sample temperature can be estimated assuming that all the heat is exchanged by radiation; therefore, the power balance can be written as [2,4,22]:

$$EJV = \sigma\varepsilon S\left(T_S^4 - T_F^4\right) \quad (2)$$

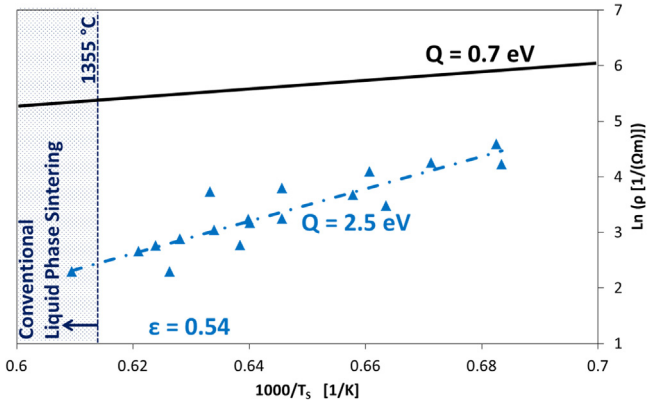

Fig. 9. Resistivity as a function of sample temperature during flash sintering (MgGCA), assuming an emissivity of 0.54. The black continuous line represents the extrapolation at high temperature of the resistivity measured before flash sintering, using the data collected at 500 – 1250 V/cm (Q = 0.7 eV). The dashes-dot line is the fitting curve, obtained with an activation energy of 2.5 eV. All but one of the points correspond to sample temperatures lower than the liquidus of the ternary system (1355 °C).

where E is the field, J the current density, V and S the sample volume and surface, respectively, σ the Stefan- Boltzmann universal constant, ε the material emissivity and T_F the furnace temperature.

The experimental data were fitted using different emissivity values in the 0.2–1 range. The best fit was obtained using an emissivity of 0.54 and an activation energy of 2.5 eV. It is possible to specify that the estimated emissivity is in the range of the data available in the literature (0.4–0.8) [38–40]. Conversely, the activation energy is much higher than that previously calculated from the power dissipation plots (0.7 eV). Even by changing the emissivity in a wide range (0.2–1), the activation energy is always higher than 1.1 eV, not comparable with the results obtained previously. In addition, one can observe that the estimated activation energy for conduction during FS in MgGCA (2.5 eV) is far higher than that calculated in previous studies for pure alumina (0.76 eV) [22].

Therefore, it is possible to state that:

i The conduction behaviour during FS is different from that observed before the current limit is reached.
ii The conduction mechanisms during FS in pure alumina and glass-containing alumina are undoubtedly different, and this suggests that the vitreous phase is mainly involved in the charge transport mechanisms.

The activation energy for conduction during flash sintering is compatible with ion diffusion phenomena in molten silicates: values in the 1.1–2.9 eV range have been previously reported for Si^{4+}, Mg^{2+} and O^{2-} diffusion [31,33,41–44]. One can observe that this value is far lower than the band gap for electron promotion in fused silica and alumina [34]. Therefore, the current is flowing in the vitreous phase during FS and, probably, the conduction is based on ionic diffusion.

In order to verify the presence of ionic conduction phenomena in the foregoing flash sintering experiments, the concentration profiles of Mg and Al were recorded by EDS close to the cathode and the anode of some FS specimens. Fig. 10 shows the data collected on the sample treated with 2 mA/mm^2 and 750 V/cm. One can see that the relative concentration of Mg is much higher at the cathode and progressively decreases moving away from the electrode, reaching a plateau after about 700 μm. Conversely, a lower Mg concentration was measured around the anode. In this case, the Mg signal increases with the distance from the electrode and it hits a constant value after about 250 μm. At larger distances the Mg concentration

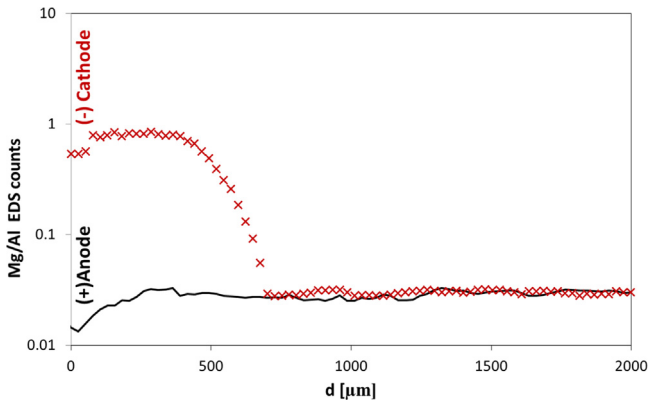

Fig. 10. Ratio between magnesium and aluminum EDS counts at different distances from anode (crosses) and cathode (continuous line) in the sample treated with 750 V/cm and 2 mA/mm^2.

does not change significantly. The asymmetry in Mg concentration is indeed a result of the DC polarization, which leads to the segregation of positive Mg^{++} ions close to the negative electrode. This phenomenon should not be observed in AC polarization.

Mg diffusion was also analysed by recording some EDS concentration maps near the cathode. As shown in Fig. 11, a strong magnesium signal was recorded very close to the electrode: a homogeneous and thin Mg-reach layer around the hole where the platinum wire was inserted is visible. By increasing the field ($E \geq 1000$ V/cm), the magnesium-enriched zone becomes wider.

No significant Si^{4+} diffusion was observed by EDS. As shown in Fig. 11, silicon concentration is always constant. This result is not surprising: since silicon is a glass network former, its mobility in molten silicates is very low. In particular, previous studies have pointed out that the diffusivity of Si^{4+} in glasses and silicates is lower when compared with other species like oxygen anions [30,33,45]. Even if in silicate minerals the diffusion coefficient of Mg^{2+} should be higher than oxygen ions [41], partial contribution of O^{2-} motion to conduction cannot be excluded.

Fig. 9 also shows a comparison between the resistivity measured during FS and an extrapolation of the resistivity behaviour observed before FS. It is possible to state that the resistivity during FS is much lower than that expected by previous measurements. This can be accounted for by the activation of different conduction mechanisms (i.e. diffusion paths with higher activation energy) during flash sintering, as a result of the increased sample temperature. Also a decrease in glass viscosity could be proposed as a possible explanation for this behaviour, in agreement with the electric field-induced softening observed by McLaren et al. [24].

In addition, in Fig. 9 one can observe that the estimated temperature reached by the samples is practically always lower than the lower liquidus temperature (1355 °C) of the ternary system Al_2O_3–SiO_2–MgO. Below this temperature it is impossible to obtain conventional efficient liquid phase sintering. In fact, the glassy phase would undergo a rather fast devitrification process, leading to the formation of a crystalline solid. In order to verify this statement, a MgGCA sample was conventionally sintered at 1350 °C for 2 h (heating rate = 10 °C/min); the sintering temperature was therefore very close to the liquidus temperature of the ternary system. A very porous microstructure was obtained as shown in Fig. 12, having quite different features from those reported in Figs. 4 and 5. In particular, a much higher amount of pores can be observed in the conventionally treated sample. This is also confirmed by density measurements, which indicate a bulk density of 2.99 g/cm^3 and an amount of open porosity higher than 13% for the sample sintered without field. The formation of Mullite and of a magnesium-aluminum silicate (Sapphirine) from the glassy phase was determined by XRD analysis. Therefore, in the conventional sintering process, the glassy phase crystallizes; being the system at a temperature lower than the liquidus, this leads to the formation of a solid second phase. The absence of a stable liquid results in a non-efficient sintering process and densification is not particularly enhanced by the addition of glass.

Therefore, by applying an external E-field it is possible to obtain an effective liquid phase sintering at sample temperatures that do not allow it by conventional methods, even after several hours. This suggests that the current flow or the rapid heating obtained by Joule effect during FS accelerates the densification phenomena more than the crystallization of the glass. In this way, an efficient and ultra-fast liquid phase sintering of the MgGCA material can be obtained at temperatures lower than the liquidus.

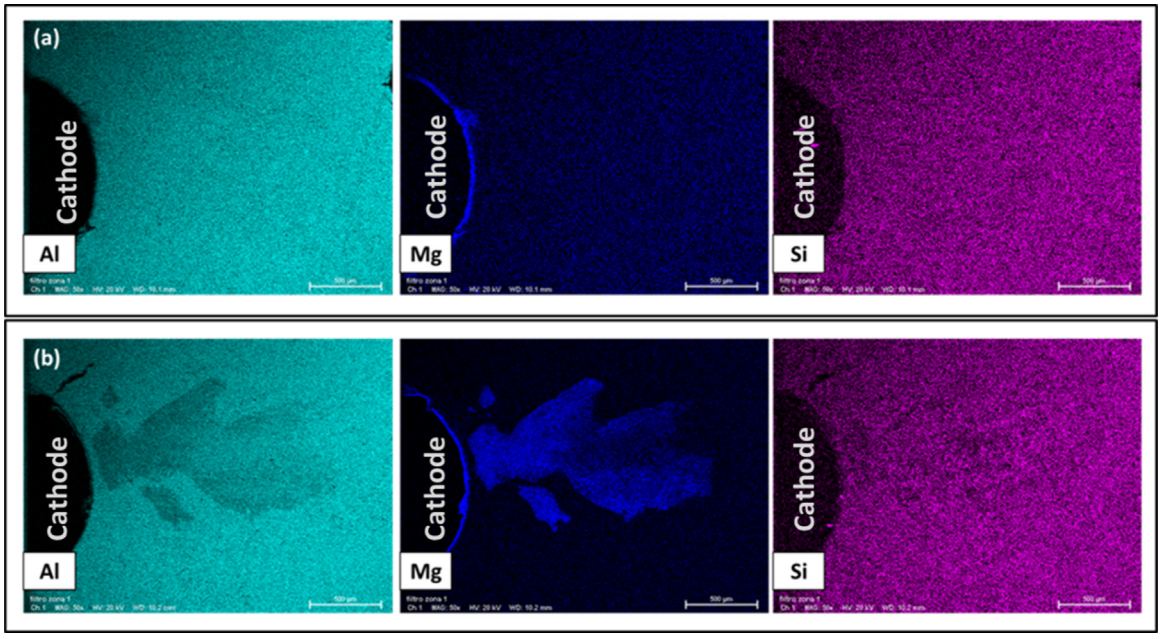

Fig. 11. EDS concentration map for Al, Mg and Si close to the cathode of sample treated with 2 mA/mm^2 under 500 (a) and 1000 V/cm (b).

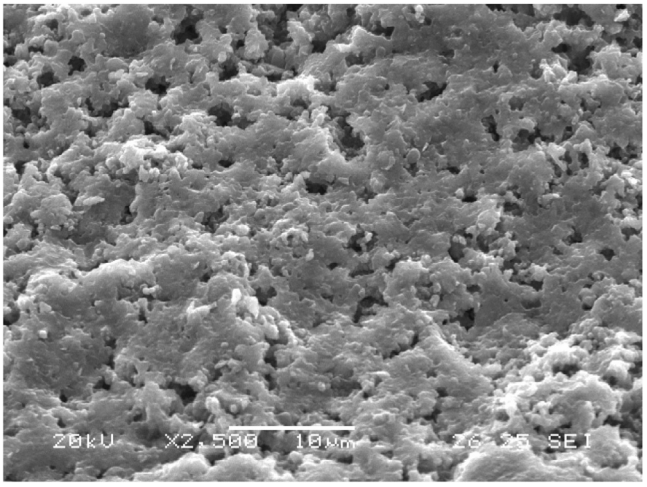

Fig. 12. SEM micrograph of a conventionally sintered magnesia-silicate glass-containing sample (T = 1350 °C, t = 2 h).

4. Conclusions

The main conclusions of the present work are:

I Flash sintering can be successfully applied to materials characterized by the simultaneous presence of glassy and crystalline phase, under the condition that the material is enough conductive: i.e., while magnesia-silicate glass-containing alumina can be easily flash sintered, pure silica glass-containing alumina never reproduces the flash event.

II The addition of magnesia-silicate glass has a beneficial role on field assisted sintering behaviour of alumina. In particular, glass containing-alumina sintered bodies are denser and characterized by lower open porosity with respect to pure alumina. This also means that one can reduce the current density and power dissipation needed for densification.

III The E-field application lowers the softening temperature of the magnesia-silicate glassy phase, anticipating the particles rearrangement phenomena. However, the shrinkage related to this stage of the liquid phase sintering is, as first approximation, independent from the field. Conversely, the applied field/current have a huge effect on densification leading to an abrupt increase of the sintering rate.

IV Power dissipation plots for magnesia-silicate glass-containing alumina bodies show an unexpected change in the curvature, probably caused by partial crystallization of the glassy phase. This results in a “non-regular” relation between the onset temperature for flash sintering and the field strength.

V The activation energy for conduction during FS is compatible with ionic diffusion in molten silicates. In particular, magnesium migration toward the cathode was observed.

VI Via E-Field application it is possible to obtain effective liquid phase sintering at sample temperatures lower than the liquidus of the corresponding ternary system.

References

[1] J.A. Downs, V.M. Sglavo, Electric field assisted sintering of cubic zirconia at 390 °C, J. Am. Ceram. Soc. 96 (2013) 1342–1344.
[2] M. Cologna, B. Rashkova, R. Raj, Flash sintering of nanograin zirconia in <5 s at 850 °C, J. Am. Ceram. Soc. 93 (2010) 3556–3559.
[3] J.S.C. Francis, Rishi Raj, Flash-Sinterforging of nanograin zirconia: field assisted sintering and superplasticity, J. Am. Ceram. Soc. 95 (2012) 138–146.
[4] R.I. Todd, E. Zapata-Solvas, R.S. Bonilla, T. Sneddon, P.R. Wilshaw, Electrical characteristics of flash sintering: thermal runaway of Joule heating, J. Eur. Ceram. Soc. 35 (2015) 1865–1877.
[5] J.S.C. Francis, M. Cologna, R. Raj, Particle size effects in flash sintering, J. Eur. Ceram. Soc. 32 (2012) 3129–3136.
[6] R. Muccillo, E.N.S. Muccillo, An experimental setup for shrinkage evaluation during electric field-assisted flash sintering: application to yttria-stabilized zirconia, J. Eur. Ceram. Soc. 33 (2013) 515–520.
[7] R. Muccillo, M. Kleitz, E.N.S. Muccillo, Flash grain welding in yttria stabilized zirconia, J. Eur. Ceram. Soc. 31 (2011) 1517–1521.
[8] R. Baraki, S. Schwarz, O. Guillon, Effect of electrical field/current on sintering of fully stabilized zirconia, J. Am. Ceram. Soc. 95 (2012) 75–78.
[9] R. Raj, M. Cologna, J.S.C. Francis, Influence of externally imposed and internally generated electrical fields on grain growth, diffusional creep sintering and related phenomena in ceramics, J. Am. Ceram. Soc. 94 (2011) 1941–1965.
[10] S.K. Jha, R. Raj, The effect of electric field on sintering and electrical conductivity of titania, J. Am. Ceram. Soc. 97 (2014) 527–534.
[11] X. Hao, Y. Liu, Z. Wang, J. Qiao, K. Sun, A novel sintering method to obtain fully dense gadolinia doped ceria by applying a direct current, J. Power Sources 210 (2012) 86–91.
[12] M. Biesuz, G. Dell'Agli, L. Spiridigliozzi, C. Ferone, V.M. Sglavo, Conventional and field-assisted sintering of nanosized Gd-doped ceria synthesized by co-precipitation, Ceram. Int. 42 (2016) 11766–11771.
[13] R. Muccillo, E.N.S. Muccillo, M. Kleitz, Densification and enhancement of the grain boundary conductivity of gadolinium-doped barium cerate by ultra-fast flash grain welding, J. Eur. Ceram. Soc. 32 (2012) 2311–2316.
[14] E. Zapata-Solvas, S. Bonilla, P.R. Wilshaw, R.I. Todd, Preliminary investigation of flash sintering of SiC, J. Eur. Ceram. Soc. 33 (2013) 2811–2816.
[15] K.S. Naik, V.M. Sglavo, R. Raj, Flash sintering as a nucleation phenomenon and a model thereof, J. Eur. Ceram. Soc. 34 (2014) 4063–4067.
[16] K.S. Naik, V.M. Sglavo, R. Raj, Field assisted sintering of ceramic constituted by alumina and yttria stabilized zirconia, J. Eur. Ceram. Soc. 34 (2014) 2435–2442.
[17] E. Bichaud, J.M. Chai, C. Carry, M. Kleitz, M.C. Steil, Flash sintering incubation in Al_2O_3/TZP composites, J. Eur. Ceram. Soc. 35 (2015) 2587–2592.
[18] A. Gaur, V.M. Sglavo, Flash-sintering of $MnCo_2O_4$ and its relation to phase stability, J. Eur. Ceram. Soc. 34 (2014) 2391–2400.
[19] A.L.G. Prette, M. Cologna, V.M. Sglavo, R. Raj, Flash-sintering of Co2MnO4 spinel for solid oxide fuel cell applications, J. Power Sources 196 (2011) 2061–2065.
[20] A. Gaur, V.M. Sglavo, Densification of $La_{0.6}Sr_{0.4}Co_{0.2}Fe$ $0.8O_3$ ceramic by flash sintering at temperature less than 100 °C, J. Mater. Sci. 49 (2014) 6321–6332.
[21] M. Cologna, J.S.C. Francis, R. Raj, Field assisted and flash sintering of alumina and its relationship to conductivity and MgO-doping, J. Eur. Ceram. Soc. 31 (2011) 2827–2837.
[22] M. Biesuz, V.M. Sglavo, Flash sintering of alumina: effect of different operating conditions on densification, J. Eur. Ceram. Soc. 36 (2016) 2535–2542.
[23] Y. Zhang, J. Jung, J. Luo, Thermal runaway, flash sintering and asymmetrical microstructural development of ZnO and ZnO-Bi2O3 under direct currents, Acta Mater. 94 (2015) 87–100.
[24] C. McLaren, W. Heffner, R. Tessarollo, R. Raj, H. Jain, Electric field-induced softening of alkali silicate glasses, Appl. Phys. Lett. 107 (2015) 184101.
[25] U. Scipioni Bertoli, Electrical Field Assisted Viscous Flow in Soda Alumina Silicate Glass, Unpublished Work, Master Thesis in Materials Engineering, University of Trento, 2012.
[26] M.N. Rahaman, Ceramic Processing and Sintering, Marcell Dekker, New York, USA, 2003.
[27] J. Gonzalez-Julian, O. Guillon, Effect of electric Field/Current on liquid phase sintering, J. Am. Ceram. Soc. 98 (2015) 2018–2027.
[28] I.-J. Bae, S. Baik, Abnormal grain growth of alumina, J. Am. Ceram. Soc. 80 (1997) 1149–1156.
[29] R. Freer, Diffusion in silicate minerals and glasses: a data digest and a guide to the literature, Contr. Mineral. Petrol. 76 (1981) 440–454.
[30] D.J. Cherniak, Diffusion in quartz melilite, silicate perovskite, and mullite, Rev. Mineral. Geochem. 72 (2010) 735–756.
[31] T. Dunn, Cation diffusion in olivine. cobalt and magnesium, M. Morioka, Geochim. Cosmochim. Acta 46 (1982) 2293–2299.
[32] H. Bracht, E.E. Haller, R. Clark-Phelps, Silicon self-diffusion in isotope heterostructures, Phys. Rev. Lett. 81 (1998) 393–396.
[33] Y. Oishi, R. Terai, H. Ueda, Oxygen diffusion in liquid silicates and relation to their viscosity, in: Material Science Research, Volume 9 Mass Transport Phenomena in Ceramics, Plenum Press, New York, USA, 1975.
[34] C. Barry Carter, M. Grant Norton, Ceramic Materials: Science and Engineering, Springer, 2007, pp. 532–533.
[35] K. Sunder, M. Grofmeier, R. Staskunaite, H. Bracht, Dynamics of network formers and modifiers in mixed cation silicate glasses, J. Phys. Chem. 224 (2010) 1677–1705.
[36] R.H. Doremus, Glass Science, Wiley, New York USA, 1994.
[37] R.J. Maurer, Deviations from ohm's law in soda lime glass, J. Chem. Phys. 9 (1941) 579–584.
[38] http://www.engineering.com/Library/ArticlesPage/tabid/85/ArticleID/151/Emissivity.aspx.
[39] E.C. Guyer, Handbook of Applied Thermal Design, Hamilton Ptrinting, Castleton, NY, USA, 1999, pp. 1–89.
[40] F. Kreith, The CRC Handbook of Thermal Engineering, CRC Press LLC, Danvers, USA, 2000, pp. 3–71.

[41] Y. Zhang, H. Ni, Y. Chen, Diffusion in silicate melts, Rev. Mieral. Geochem. 72 (2010) 311–408.
[42] E.L. Williams, Diffusion of oxygen in fused silica, J. Am. Ceram. Soc. 48 (1965) 190–194.
[43] Y. Zhang, H. Ni, Diffusion of H, C and O components in silicate melts, Rev. Mineral. Geochem. 72 (2010) 171–255.
[44] C.E. Lesher, R.L. Hervig, D. Tinker, Self diffusion of network formers (silicon and oxygen) in naturally occurring basaltic liquid, Geochim. Cosmochim. Acta 60 (1996) 405–413.
[45] H.A. Shaeffer, Transport phenomena and diffusion anomalies in glass, Ceram. Mater. 64 (2012) 156–161.